Spatial model of autocatalytic reactions

Pietro de Anna

Géosciences Rennes, UMR 6118, CNRS, Université de Rennes 1, Rennes, France

Francesca Di Patti

Dipartimento di Fisica "Galileo Galilei," Università degli Studi di Padova, via F. Marzolo 8, 35131 Padova, Italy

Duccio Fanelli

Dipartimento di Energetica, University of Florence and INFN, Via S. Marta 3, 50139 Florence, Italy

Alan J. McKane

Theoretical Physics, School of Physics and Astronomy, University of Manchester, Manchester M13 9PL, United Kingdom

Thierry Dauxois

Université de Lyon, Laboratoire de Physique de l'École Normale Supérieure de Lyon, CNRS, France

Biological cells with all of their surface structure and complex interior stripped away are essentially vesicles—membranes composed of lipid bilayers which form closed sacs. Vesicles are thought to be relevant as models of primitive protocells, and they could have provided the ideal environment for prebiotic reactions to occur. In this paper, we investigate the stochastic dynamics of a set of autocatalytic reactions, within a spatially bounded domain, so as to mimic a primordial cell. The discreteness of the constituents of the autocatalytic reactions gives rise to large sustained oscillations even when the number of constituents is quite large. These oscillations are spatiotemporal in nature, unlike those found in previous studies, which consisted only of temporal oscillations. We speculate that these oscillations may have a role in seeding membrane instabilities which lead to vesicle division. In this way synchronization could be achieved between protocell growth and the reproduction rate of the constituents (the protogenetic material) in simple protocells.

PACS number(s): 82.20.−w, 02.50.Ey, 05.40.−a, 87.16.dj

I. INTRODUCTION

The cell is a structural and functional unit, the building block of any living system. Cells consist of a membrane, made of a lipid bilayer, which encloses and protects the contents of the cell, including genetic material. The membrane is semipermeable: nutrients can diffuse in and serve as energy to support the functioning of the machinery [1]. Cells undergo replication (cell division): this is a process by which a cell, hereafter called the parent cell, divides into two or more cells, called the daughters. The daughter cell contains in principle an exact replica of the parent's inner constituents, this property being ultimately a prerequisite for stable living organisms to exist. Such a process clearly relies on the synchronization between the duplication rate of the constituents and the growth of the container. In modern cells this condition is of paramount importance and is efficiently realized via dedicated control mechanisms, expressed as pathways of nested molecular checkpoints [1]. This complex and delicate machinery has evolved; presumably the first minimalistic cells (so-called protocells [2–10]) had a far more straightforward and less elaborate way of dividing. So focusing on the primordial cell units postulated to be present at the origin of life on Earth, can we conceive of a simple, though efficient, mechanism which could govern the division process? A possible answer to this question will emerge as a result of the calculations carried out in this paper.

One of the most persuasive scenarios concerning the origin of life on Earth identifies vesicles as protocells [11].

These are tiny closed sacs in which the outer membrane takes the form of a lipid bilayer and so are good candidates for a minimal cell. Despite the dramatic reduction in complexity as compared to modern cells, vesicles still display many fascinating properties, as revealed in laboratory experiments [11,12]. They are semipermeable and allow for different types of chemicals to enter the enclosed volume, and so sustain any reaction cycles that may be taking place. In addition, vesicles can grow due to inclusion of lipid constituents into their surface, progressively adjust their shape, and eventually divide to produce daughter vesicles. Vesicles which are initially spherical can pass through a number of intermediate shapes before they divide, for instance a vesicle may first change into an ellipsoid, then into a dumbbell shape and finally into two attached spheres, at which point it will divide in two [12].

However it must be said there is in reality very little theoretical evidence that the shape of the vesicle always follows this particular sequence and even less experimental evidence. It may be more appropriate to talk about an ensemble of vesicles and typical pathways to the state where division takes place. Similarly there may only be a mean time to division, although it should be noted that there would then be a selection process which would favor the types of vesicles (if they could be distinguished) which would undergo the division proceeding at the fastest rate.

When modeling protocells, one needs to relate the mechanism of growth and division to the actual microscopic dynamics of the internal constituents. While vesicles can pos-

sibly define the scaffold of prototypical cell models, what can one say about the internal constituents? It is customarily believed that autocatalytic reactions [13] might have had a role in producing complex molecules required for the origin of life [14–17]. A chemical reaction is called autocatalytic if one of the reaction products is itself a catalyst for the chemical reaction. Clearly the reaction will speed up as more catalyst is produced. If there are several catalytic reactions, rather than just one—an autocatalytic set [18]—then more complex behavior is possible, with some reactions producing catalysts for other reactions. This suggests that the interior of the protocell might have been occupied by interacting families of replicators, organized in autocatalytic cycles.

Autocatalytic reactions have also been invoked in the context of studies on the origin of life as a possible solution of the famous Eigen paradox [19]. This is a puzzle, since it limits the size of self-replicating molecules to perhaps a few hundred base pairs. At odds with this conclusion, almost all life on Earth requires much longer molecules to encode their genetic information. This problem is dealt with in living cells by the presence of enzymes which repair mutations, allowing the encoding molecules to reach sizes on the order of millions of base pairs [20]. In primordial organisms, autocatalytic cycles might have provided the required degree of microscopic cooperation to prevent Eigen's evolutionary drive to self-destruction to occur.

In this paper we will investigate the properties of autocatalytic reactions within a bounded region of space, which we will identify with the vesicle, the whole structure being a reference model for a protocell. The autocatalytic reactions will be taken to have the form proposed by Togashi and Kaneko [21,22]. In their work, Togashi and Kaneko emphasized the role played by the noise intrinsic to the system of elementary constituents. This model was recently revisited by Dauxois *et al.* [23], who used an approach based on expanding the master equation in a system-size expansion [24], to make analytic progress in the description of the process. This approach has recently been applied to a number of processes in biological systems to show how large oscillations can emerge, sustained by the stochastic component of the dynamics [25–27]. The analysis has also been extended to a spatial model [28], and our calculations will mirror those in this paper.

Therefore here we will ask what happens once space (i.e., microscopic particle diffusion) is incorporated into the model. Are the oscillations robust or, conversely, do they get washed out through coarse-grained averaging? We shall demonstrate that spatiotemporal patterns do emerge and influence the mass transport inside the cell. We will also speculate that the division of the protocell requires an inherent degree of synchronization which may be triggered by collective, spatially ordered fluctuations in the concentration. Building on this scenario, one can imagine that localized peaks in the concentration might develop at a given stage of the vesicle evolution. Denser patches could then drive an instability which could potentially lead to the distortion of the membrane and so to division.

II. MODEL

The model we will use is a spatial version of the autocatalytic model discussed in [23]. The idea is to introduce a
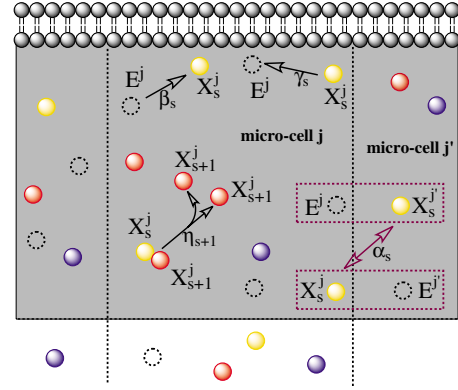

FIG. 1. (Color online) The volume of the cells adjacent to the boundary is imagined to be partitioned into Ω microcells (see also Fig. 2). Within microcell j the molecular species interact according to the autocatalytic reactions specified by Eqs. (1). In addition, the molecules can migrate from microcell j to its nearest neighbors, e.g., microcell j', as depicted in the cartoon. A molecule of type X_s^j (full circle) takes over a vacancy (dashed empty circle) of microcell $E^{j'}$, and so transforms into $X_s^{j'}$, leaving behind a vacancy E^j. Finally, the chemical can also diffuse in from the environment, a reaction that in turn implies changing E^j into X_s^j. The opposite holds for molecules that diffuse out into the environment.

spatial coarse-graining and divide the vesicle into small microcells, within which autocatalytic reactions occur. The cells adjoining the membrane which forms the limit of the vesicle have a special status, since the membrane allows chemicals to diffuse in from the environment and out into the environment. In this paper we will focus only on these microcells—those that are adjacent to the boundary—and lump all the interior microcells together into an inner region. We do not give the environment or this inner region any spatial structure; they simply act as a particle reservoir for the chemicals in the microcells adjacent to the membrane.

In each microcell autocatalytic reactions as specified in [23] occur, see Fig. 1. More specifically we consider k chemical species, here labeled X_s^j, with the index s $= 1, \ldots, k$ labeling the species and $j = 1, \ldots, \Omega$, the Ω microcells where the reactions occur. The autocatalytic reactions take the form [23]

$$X_s^j + X_{s+1}^j \xrightarrow{\eta_{s+1}} 2X_{s+1}^j. \tag{1}$$

The reactions are taken to be cyclic so that $X_{k+1}^j = X_1^j$.

The spatial element of the model is introduced through migration of chemical species between neighboring cells. The boundary cells will form a periodic structure in two dimensions so that a Fourier-based approach can be used in the analysis described below. The geometry is schematically depicted in Fig. 2, in a two-dimensional setting, so that the microcells form a one-dimensional periodic structure. It should be emphasized that although the scheme is illustrated in Fig. 2 with reference to a two-dimensional vesicle for simplicity, the setting and analysis apply in any spatial dimension including the relevant three-dimensional case. If the vesicle is $d+1$ dimensional, clearly the microcells will form a d-dimensional periodic structure.
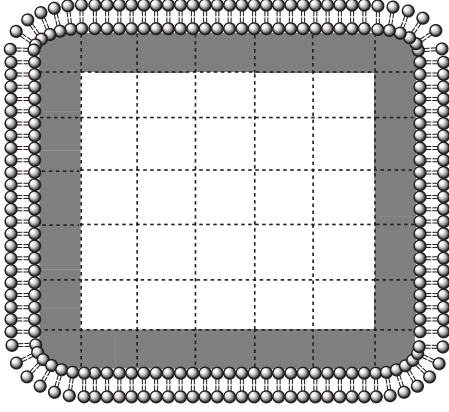
FIG. 2. In the spatial autocatalytic model considered here the vesicle is imagined to be divided into small microcells. We are specifically interested in the microcells adjoining the membrane, shown in darker outline in the figure. These latter link up together and constitute a sort of inner shell, immediately adjacent to the vesicle wall. Within each microcell the chemicals interact as shown in Fig. 1.

The migration between adjacent cells is encapsulated in the following relations:

$$X_s^j + E^{j'} \xrightarrow{\alpha_s} X_s^{j'} + E^j, \qquad (2)$$

$$E^j + X_s^{j'} \xrightarrow{\alpha_s} E^{j'} + X_s^j, \qquad (3)$$
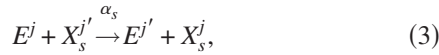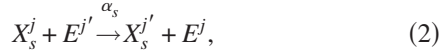
where j and j' label the adjacent cells and E^i represents vacancies in cell i. We will assume that the capacity of each cell is N, so that sum of the number of molecules of each species plus the number of vacancies equals N for every cell.

Finally, cell j may lose a molecule X_s^j to the environment or inner region leaving a vacancy E^j or a gain of a molecule X_s^j from the environment or inner region, i.e.,

$$X_s^j \xrightarrow{\gamma_s} E^j; \quad E^j \xrightarrow{\beta_s} X_s^j. \qquad (4)$$
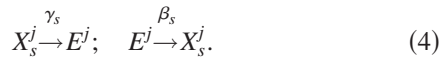
There is no need to distinguish between the environment and inner region; the rates γ_s and β_s can simply be regarded as the combined rates for both processes. In the rest of the paper we will simply refer to both these regions as "the environment."

In the following we will formulate the model in terms of a chemical master equation and find the mean-field solution as well as determining stochastic corrections to this which occurs when N is finite. We will also simulate the stochastic dynamics and compare the results with the analytic formulas we obtain.

To describe the model as a chemical master equation, we denote the number of molecules of chemical species s in cell j by n_s^j, and so the state of the system can be characterized by the vector $\mathbf{n} = (\mathbf{n}^1, \mathbf{n}^2, \ldots, \mathbf{n}^\Omega)$ where $\mathbf{n}^j = (n_1^j, n_2^j, \ldots, n_k^j)$. The transition rate from one state $\mathbf{n}'$, to another $\mathbf{n}$, is denoted by $T(\mathbf{n}|\mathbf{n}')$—with the initial state being on the right. For example, the transitions stemming from the autocatalytic cycles are

$$T(n_s^j - 1, n_{s+1}^j + 1 | n_s^j, n_{s+1}^j) = \frac{\eta_{s+1}}{\Omega} \frac{n_s^j}{N} \frac{n_{s+1}^j}{N}, \qquad (5)$$

where within the brackets we have chosen to indicate only the dependence on those species which are involved in the reaction. The transition rates associated with the migration between adjacent microcells take the form

$$T(n_s^j - 1, n_s^{j'} + 1 | n_s^j, n_s^{j'}) = \frac{\alpha_s}{z\Omega} \frac{n_s^j}{N} \left(1 - \sum_{m=1}^k \frac{n_m^{j'}}{N} \right),$$

$$T(n_s^j + 1, n_s^{j'} - 1 | n_s^j, n_s^{j'}) = \frac{\alpha_s}{z\Omega} \frac{n_s^{j'}}{N} \left(1 - \sum_{m=1}^k \frac{n_m^j}{N} \right), \qquad (6)$$

where z is the number of nearest neighbors that each microcell has. Finally, for the interaction with the environment, the transition rates are

$$T(n_s^j - 1 | n_s^j) = \frac{\gamma_s}{\Omega} \frac{n_s^j}{N},$$

$$T(n_s^j + 1 | n_s^j) = \frac{\beta_s}{\Omega} \left(1 - \sum_{m=1}^k \frac{n_m^j}{N} \right). \qquad (7)$$

In Eqs. (6) and (7), explicit use has been made of the condition

$$\sum_{s=1}^k \frac{n_s^j}{N} + \frac{n_E^j}{N} = 1, \qquad (8)$$

to eliminate n_E^j, the number of vacancies in cell j.

The system is intrinsically stochastic and may be described by the probability density function, $P(\mathbf{n}, t)$, which gives the probability of finding the system in state $\mathbf{n}$ at time t. The equation which governs the dynamical evolution of $P(\mathbf{n}, t)$ is the master equation [24], which for the system under consideration here takes the form

$$\frac{dP(\mathbf{n}, t)}{dt} = \sum_{j=1}^\Omega \mathcal{T}_{\text{loc}}^j P(\mathbf{n}, t) + \sum_{j=1}^\Omega \sum_{j' \in j} \mathcal{T}_{\text{mig}}^{jj'} P(\mathbf{n}, t)$$
$$+ \sum_{j=1}^\Omega \mathcal{T}_{\text{env}}^j P(\mathbf{n}, t), \qquad (9)$$

where the three terms on the right-hand side refer to the local terms for the chemical reactions, the migration of chemical species between the microcells, and the interaction with the environment, respectively. The notation $j' \in j$ means that the cell j' is a nearest-neighbor of the cell j. The three terms in the master equation can be expressed in a concise, but transparent, form by introducing the step operator [24] $\mathcal{E}_{s,j}^{\pm 1}$ defined by

$$\mathcal{E}_{s,j}^{\pm 1} f(\{n_m^i\}) = f(\ldots, n_s^j \pm 1, \ldots), \qquad (10)$$

where f is an arbitrary function. The explicit forms for these three terms are

$$T^j_{\text{loc}} = \sum_{s=1}^{k} (\mathcal{E}_{s,j} \mathcal{E}^{-1}_{s+1,j} - 1) T(n^j_s - 1, n^j_{s+1} + 1 | n^j_s, n^j_{s+1}), \quad (11)$$

$$T^{jj'}_{\text{mig}} = \sum_{s=1}^{k} (\mathcal{E}_{s,j} \mathcal{E}^{-1}_{s,j'} - 1) T(n^j_s - 1, n^{j'}_s + 1 | n^j_s, n^{j'}_s)$$
$$+ \sum_{s=1}^{k} (\mathcal{E}_{s,j'} \mathcal{E}^{-1}_{s,j} - 1) T(n^{j'}_s - 1, n^j_s + 1 | n^{j'}_s, n^j_s), \quad (12)$$

$$T^j_{\text{env}} = \sum_{s=1}^{k} [(\mathcal{E}_{s,j} - 1) T(n^j_s - 1 | n^j_s) + (\mathcal{E}^{-1}_{s,j} - 1) T(n^j_s + 1 | n^j_s)],$$
$$(13)$$

where it is understood that the operator $\mathcal{E}^{\pm 1}_{s,j}$ also acts on $P(\mathbf{n}, t)$ when these expressions are substituted into Eq. (9). In Eq. (11) the cyclic nature of the reactions means that n^j_{k+1} should be identified as n^j_1 and $\mathcal{E}^{\pm 1}_{k+1,j}$ should be identified as $\mathcal{E}^{\pm 1}_{1,j}$. The explicit expressions for the transition rates are given by Eqs. (5)–(7). These, together with Eqs. (9)–(13), define the model.

The above description is exact; no approximations have yet been made. At this stage we could also resort to direct numerical simulations of the chemical reaction system by use of the Gillespie algorithm [29,30]. This method produces realizations of the stochastic dynamics which are formally equivalent to those found from the master Eq. (9). Averaging over many realizations enables us to calculate quantities of interest. We will discuss the results of performing such simulations in Sec. IV, but a very accurate approximation scheme exists which can be used to investigate models of this type analytically. This is the van Kampen system-size expansion [24]. It is effectively an expansion in powers of $N^{-1/2}$, which to leading order ($N \to \infty$) gives the deterministic equations describing the system and which at next-to-leading order gives finite N corrections to these. These latter corrections take the form of *linear* stochastic differential equations which can then be analyzed straightforwardly, especially in the case when the deterministic system has approached a stable fixed point. The method is based on substituting the ansatz

$$\frac{n^j_s}{N} = \phi^j_s + \frac{1}{\sqrt{N}} \xi^j_s, \quad (14)$$

into the master Eq. (9). Here $\phi^j_s(t)$ is the solution to the deterministic equation, and $\xi^j_s(t)$ is a stochastic term which is the difference between the actual value n^j_s/N and ϕ^j_s at time t.

We develop this approximation in the next two sections. In Sec. III we carry out the analysis to leading order, finding the deterministic equations and the relevant fixed point. In Sec. IV we carry through the calculation to next-to-leading order, investigating the linear stochastic differential equations by taking their Fourier transforms. The derivations of these equations is lengthy, though straightforward, and the details of the expansion are provided in Appendixes A and B.

III. LEADING ORDER: THE DETERMINISTIC EQUATIONS

In the limit where the number of molecules (including vacancies) in each microcell, N, goes to infinity, the system becomes deterministic and is governed by a set of ordinary differential equations. These are found by substituting the ansatz [Eq. (14)] into the master Eq. (9) and letting $N \to \infty$, after the introduction of a rescaled time $\tau = t/(N\Omega)$. The calculation is described in Appendix A, but the same equation can also be found by multiplying Eq. (9) by n^j_s and summing over all states $\mathbf{n}$. Either way one obtains the following equation for species s in cell j:

$$\frac{d\phi^j_s}{d\tau} = \eta_s \phi^j_{s-1} \phi^j_s - \eta_{s+1} \phi^j_s \phi^j_{s+1}$$
$$+ \alpha_s \left(\Delta \phi^j_s \left(1 - \sum_{m=1}^{k} \phi^j_m \right) + \phi^j_s \sum_{m=1}^{k} \Delta \phi^j_m \right)$$
$$+ \beta_s \left(1 - \sum_{m=1}^{k} \phi^j_m \right) - \gamma_s \phi^j_s, \quad (15)$$

where Δ is the discrete Laplacian operator $\Delta f^j_s = (2/z) \sum_{j' \in j} (f^{j'}_s - f^j_s)$. In the limit where the size of the microcells tends to zero, these equations become partial differential equations, with Δ becoming the familiar Laplacian operator. In this respect, Eq. (15) generalizes the results of [23] to the case of a spatially extended system. When turning off the migration mechanism between neighboring microcells, i.e., imposing $\alpha_s = 0$ for any species s, the spatial aspects drop out and one formally recovers the ordinary differential equations given in [23].

To proceed with the analysis and to make contact with the investigation carried out in [21,23], we shall now assign the same chemical parameters to all the species. The migration rate is the only exception to this, and may have a different value for each species. We will see later that this will be necessary in order to find spatiotemporal oscillations but also, as we will see shortly, a straightforward analysis is still possible if we maintain in α_s, and none of the other parameters, an explicit reference to the index s. We will be concerned with finding the homogeneous solution of Eq. (15), that is, the solution with no spatial variation. The homogeneous solution is found to be an attractor of the deterministic dynamics, even when the system is initially prepared in a nonhomogeneous configuration. This observation follows from numerical simulations but can in principle be made quantitative by investigating the stability of the homogeneous fixed point. This means that no gradient in concentration is allowed between neighboring microcells, once the asymptotic regime is attained. So, when searching for fixed points of the dynamics, one can set the terms involving the Laplacian in Eq. (15) to zero. Since the only dependence on s, appearing in α_s, multiplies these terms, there is also no dependence remaining on the species type, s, and so the fixed points are both independent of j and of s. Under these conditions a unique fixed point for the concentration, ϕ^*, is easily found to be

$$\phi^* = \frac{\beta}{k\beta + \gamma}, \tag{16}$$

for any $s = 1, \ldots, k$ and $j = 1, \ldots, \Omega$. The result [Eq. (16)] is identical to that obtained in [23] when dealing with the nonspatial homologous model.

In [23], fluctuations for finite N were shown to induce regular temporal oscillations in the species populations, so significantly altering the predicted deterministic dynamics. What is going to happen in the present spatial context? In Sec. IV we shall investigate this, the central point of the paper, by focusing on the next-to-leading order corrections in the van Kampen expansion.

IV. NEXT-TO-LEADING ORDER: THE STOCHASTIC CORRECTIONS

Equating the terms of next-to-leading order in the master equation, after rescaling the time, leads to the Fokker-Planck Eq. (B1) which governs the probability density function of the fluctuations. This Fokker-Planck equation is formally equivalent to the following Langevin equation [31,32]:

$$\frac{d\xi_s^j}{d\tau} = \sum_{j',r} M_{sr}^{jj'} \xi_r^{j'} + \lambda_s^j(\tau), \tag{17}$$

where

$$\langle \lambda_s^j(\tau) \lambda_r^{j'}(\tau') \rangle = \mathcal{B}_{sr}^{jj'} \delta(\tau - \tau'). \tag{18}$$

The noise term, $\lambda_s^j(\tau)$, in Eq. (17) is Gaussian with zero mean and with a correlator given by Eq. (18), from which it can be seen to be white. The form of the two matrices M and $\mathcal{B}$ are discussed in Appendix B. They depend on the solution of the deterministic equation $\phi_s^j(\tau)$, and so in principle are time-dependent, since ϕ_s^j is. However, in practice we are interested in fluctuations about the stationary state, ϕ^*, and so they lose their time dependence. They also only have a nontrivial spatial dependence through the presence of the discrete Laplacian because the stationary state is homogeneous. Therefore the calculation can be considerably simplified by taking the spatial Fourier transform of Eqs. (17) and (18). As discussed in Appendix B this gives (see also [28])

$$\frac{d\xi_s^{\mathbf{k}}}{d\tau} = \sum_r M_{sr}^{\mathbf{k}} \xi_r^{\mathbf{k}} + \lambda_s^{\mathbf{k}}(\tau), \tag{19}$$

where

$$\langle \lambda_s^{\mathbf{k}}(\tau) \lambda_r^{\mathbf{k}'}(\tau') \rangle = \mathcal{B}_{sr}^{\mathbf{k}} \Omega a^d \delta_{\mathbf{k}+\mathbf{k}',0} \delta(\tau - \tau'), \tag{20}$$

and where $\mathbf{k}$ is the wave vector. Here we have assumed that the microcells form a hypercubic lattice in d—dimensions with a lattice spacing a. The matrices $M^{\mathbf{k}}$ and $\mathcal{B}^{\mathbf{k}}$ are given by Eqs. (B9)–(B13) and (B15)–(B19), respectively. However the important point is that now $\mathbf{k}$ is simply a label and the matrix structure originating from the spatial nature of the problem has been lost. Thus both $M^{\mathbf{k}}$ and $\mathcal{B}^{\mathbf{k}}$ are simply $k \times k$ matrices (recall that k is the number of chemical species) and the analysis from now on is as in the nonspatial case [23].

As we have already stressed in this paper, fluctuations about the stationary state need to be taken into account since they can be significant even if N is quite large. The fact we can investigate these systematically is crucially dependent on the linearity of Eq. (19) and that the $M^{\mathbf{k}}$ and $\mathcal{B}^{\mathbf{k}}$ matrices are time independent. It means that we can straightforwardly take the temporal Fourier transform of Eq. (19) to obtain

$$\sum_{r=1}^k (-i\omega\delta_{sr} - M_{sr}^{\mathbf{k}}) \widetilde{\xi}_r^{\mathbf{k}}(\omega) = \widetilde{\lambda}_s^{\mathbf{k}}(\omega), \tag{21}$$

where $\widetilde{f}$ denotes the temporal Fourier transform of the function f. Defining the matrix $(-i\omega\delta_{sr} - M_{sr}^{\mathbf{k}})$ to be $\Phi_{sr}^{\mathbf{k}}(\omega)$, the solution to Eq. (21) is

$$\widetilde{\xi}_r^{\mathbf{k}}(\omega) = \sum_{s=1}^k [\Phi^{\mathbf{k}}(\omega)]_{rs}^{-1} \widetilde{\lambda}_s^{\mathbf{k}}(\omega). \tag{22}$$

From previous investigations, and the nature of the system, we expect that the fluctuations about the stationary state [Eq. (16)] will oscillate and will also be sustained and enhanced by a resonant effect [23,25]. This is indeed what is seen. To investigate this effect systematically we focus our attention on the power spectrum $P_s(\mathbf{k}, \omega)$ of the fluctuations of species s,

$$P_s(\mathbf{k}, \omega) \equiv \langle |\xi_s^{\mathbf{k}}(\omega)|^2 \rangle$$
$$= \Omega a^d \sum_{r=1}^k \sum_{u=1}^k [\Phi^{\mathbf{k}}(\omega)]_{sr}^{-1} \mathcal{B}_{ru}^{\mathbf{k}} [\Phi^{\mathbf{k}\dagger}(\omega)]_{us}^{-1}. \tag{23}$$

The theoretical power spectrum can be found and plotted out, for any given choice of the chemical parameters, from Eq. (23). To make contact with earlier investigations [23] and aiming at elucidating the spatial effects, we here solely focus on the choice $k = 4$ and select $\eta = 10$, $\beta = 5/32$, and $\gamma = 5/32$. When the α_s are set equal to zero, the communication between neighboring microcells is silenced, each spatial block behaving as an independent unit. Based on Eq. (23), a temporal peak in the power spectrum is predicted to occur. The peak is approximately located at $\omega \simeq 4$, in agreement with the analysis developed in [23]. Another simple limit is when the α_s are made equal for all of the k chemical species. For this choice of parameters, once again there is only a temporal peak (i.e., a global peak at $|\mathbf{k}| = k_1 = 0$). The local peak gets progressively damped as $|\mathbf{k}|$ gets larger, the effect being more pronounced the larger the values for the migration parameters. A similar phenomenon was also reported to occur in [28].

More interestingly, in Fig. 3, we show the theoretical power spectrum Eq. (23) for α_s that take different values for each of the species in the case of a two-dimensional vesicle (a one-dimensional periodic lattice of microcells, i.e., $d = 1$). The range of variation in the α_s covers several orders of magnitude, which in turn corresponds to assigning a significantly different degree of mobility to the species. Molecules characterized by large values of α_s will quickly diffuse, while those with smaller α_s are associated with relatively static and, presumably, more massive, species. A localized peak is clearly displayed suggesting that organized spa-

$P_1(\omega,k_1)$

(a)

(b) k_1

$P_2(\omega,k_1)$

(c)

(d) k_1

$P_3(\omega,k_1)$

(e)

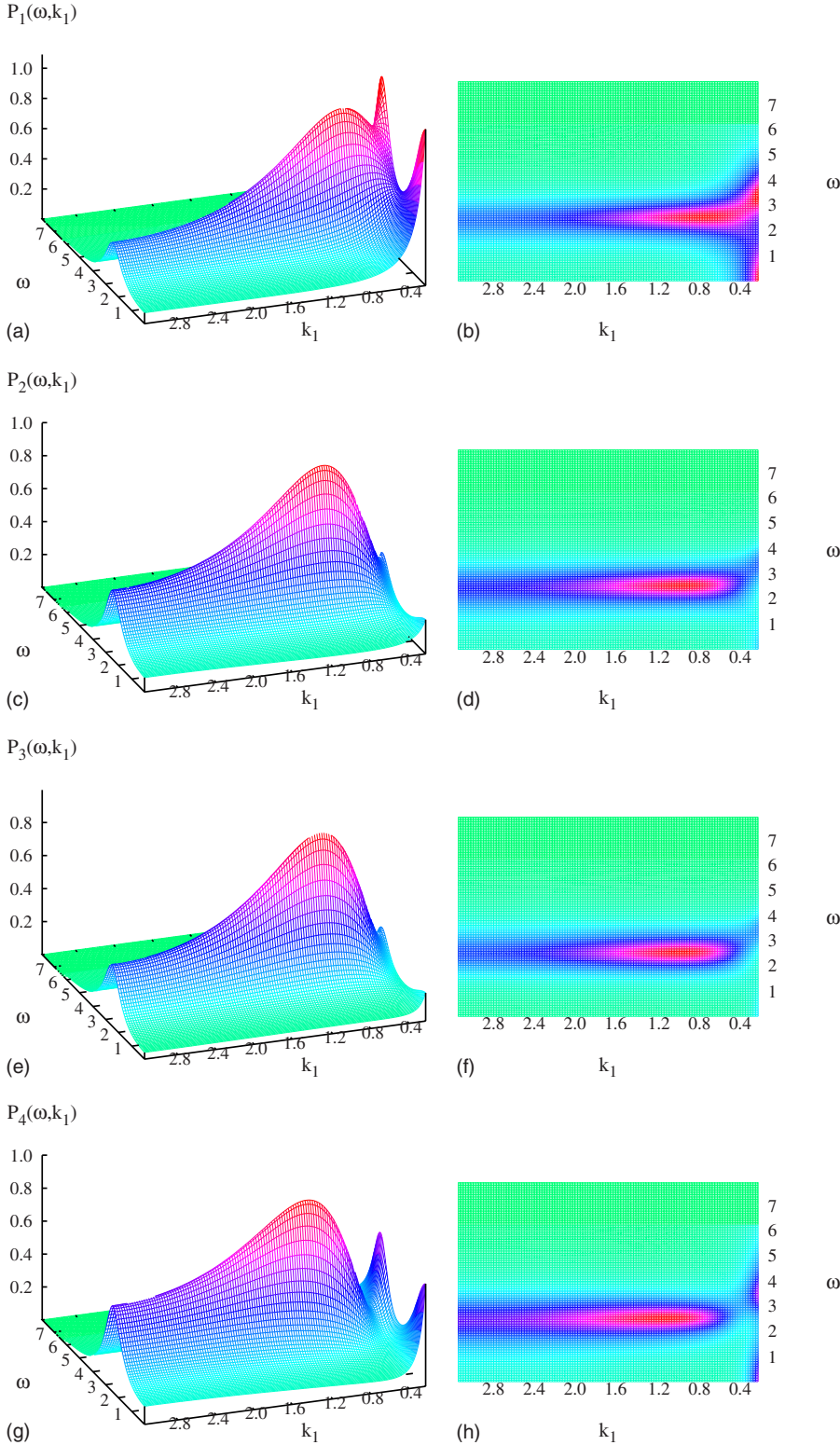(f) k_1

$P_4(\omega,k_1)$

(g)

(h) k_1

FIG. 3. (Color online) Power spectra calculated from Eq. (23) for $k=4$ species and for a two-dimensional vesicle (one-dimensional periodic array of microcells). Here $\Omega=256$, $\eta=10$, $\beta=5/32$, $\gamma=5/32$, and $\boldsymbol{\alpha}=[100,0.001,1,500]$. Each pair of panels (the three-dimensional plot and its two-dimensional projection) refers to a different chemical species. A localized peak is displayed predicting the existence of regular spatiotemporal patterns.

tiotemporal patterns can spontaneously emerge due to the inherent stochasticity of the system. From an inspection of Figs. 3, it is also evident that the power spectrum shows a clear peak for all four species. We found that making the α_s significantly different among species was a simple way to produce localized spatiotemporal patterns. We also found that they could be produced if (at least) one of the α_s was sufficiently large, when compared with the others. By con-trast, if the α_s were not too different, the global peak re-mained at $|\mathbf{k}|=k_1=0$, indicating that only temporal cycles exist in this case.

The conclusion of the above analysis, as well as the ac-curacy of the approximations that have been employed, can be tested via direct numerical simulations. By averaging over many realizations, we can calculate the power spectra after Fourier transformation. Results of the simulation are dis-
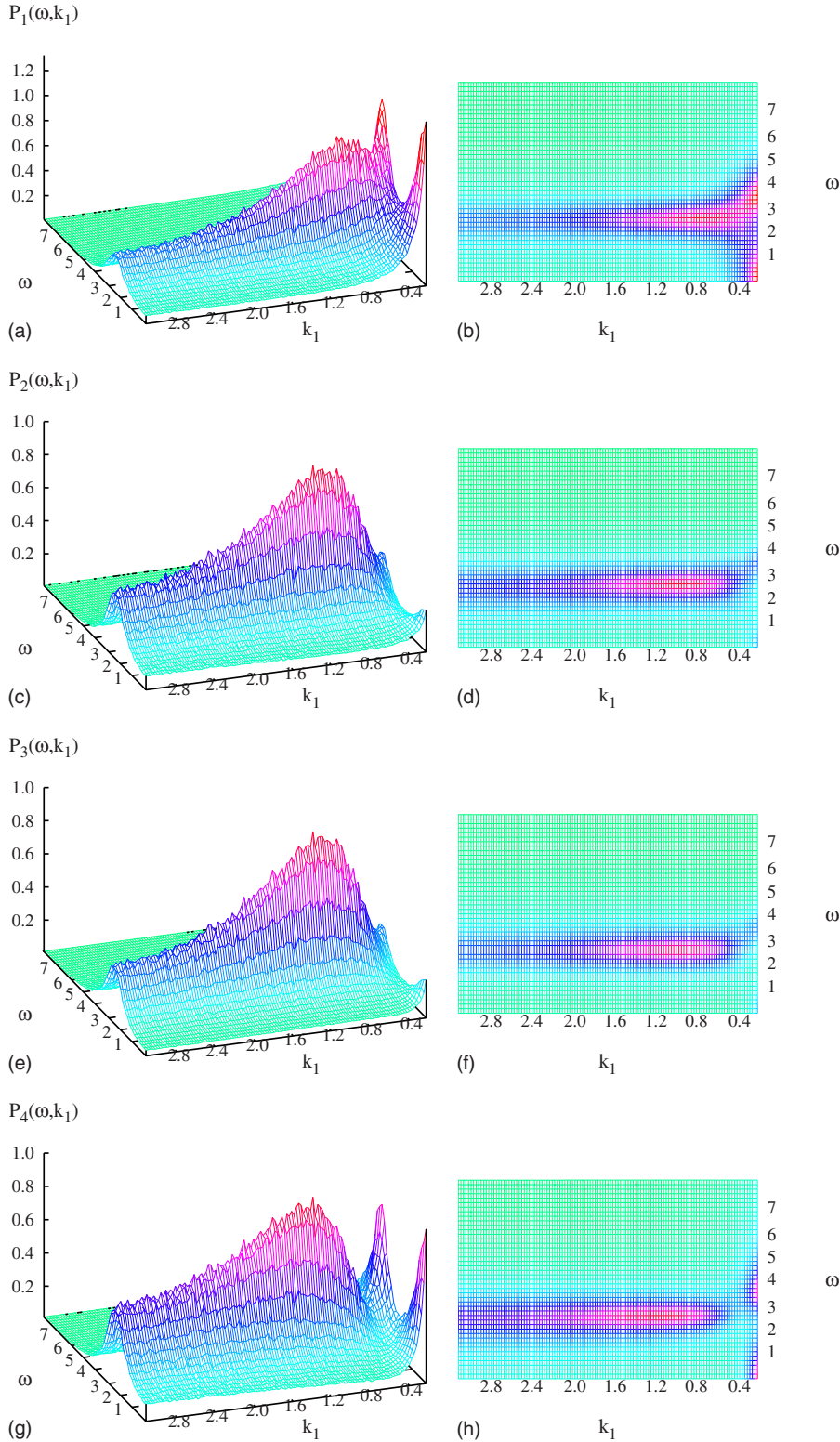
FIG. 4. (Color online) Numerically calculated power spectra obtained from averaging 800 realizations. Stochastic simulations are performed via the Gillespie algorithm. Parameters are set as in Fig. 3 and $N=5000$.

played in Fig. 4 for the same choice of parameters as in Fig. 3. The correspondence between the profiles is excellent and so confirms the correctness of our theoretical scheme.

In summary, we have unambiguously demonstrated that organized spatiotemporal cycles can emerge in a simple model of protocells where the constituents inside the vesicle interact via an autocatalytic scheme. As we shall argue in the following, this finding provides a possible mechanism to

drive a dynamical synchronization between the duplication of genetic material inside a protocell and the division of the vesicle membrane.

V. DISCUSSION

In this paper we have investigated how the discreteness of the constituents in a set of autocatalytic reactions can lead to

spatiotemporal oscillations. The occurrence of temporal oscillations in such a setting, but without a spatial element, has previously been studied [21,23]. Similarly, such oscillations have been studied for a predator-prey system in a spatial framework [28], but the oscillations in this case did not occur at a nonzero value of **k**. In this paper, we have combined and generalized these treatments, and also put them into the context of vesicles, which suggests an interesting consequence of the oscillatory behavior.

We can speculate that the natural tendency of the chemical constituents to organize in regular spatiotemporal cycles can be instrumental in achieving a degree of synchronization between the outer membrane of the vesicle and the mixture of chemicals inside. In the context of protocells, these chemicals undergoing autocatalytic reactions are to be interpreted as a primitive form of genetic material. One would expect, as a minimal self-consistency requirement, that within a stable population, a vesicle would split into two when the chemical material contained within it had approximately doubled in size. It is tempting to postulate that such a property is a dynamical phenomenon, the density fluctuations acting as a positive feedback on the vesicle growth, so signaling when the constituents inside the vesicle are ready for the splitting to take place.

Now let us imagine that the vesicle containing the chemical species grows because of the inclusion of successive membrane constituents from the environment in which it moves. Laboratory experiments indicate [11] that a vesicle filled with water or solutes is kept in a turgid spherical shape while growing by additional material of a similar kind flowing in from the outside environment. It is believed that the vesicle remains spherical until a thermodynamic instability sets in which distorts the structure [33], eventually leading to fissioning. Now suppose that the vesicle is filled by a discrete population of chemical constituents, which undergo an independent dynamics of the autocatalytic type. As illustrated in this paper, the chemicals experience a first rapid evolution toward the stationary state, where enhanced oscillations appear due to the intrinsic finiteness of the interacting constituents. Such oscillations might seed an instability which could resonate with the innate ability of the container to divide, so initiating the splitting process. A different method of seeding such an instability has been proposed by Macia and Solé [34,35]. These ideas could be extended to protocells, where enhanced oscillations could originate in the primitive genetic material. These oscillations could signal to the membrane that the genetic evolution had been virtually taken to completion and that the fission could now occur, so ensuring that the genetic material is passed on to the daughter protocells. This is a highly speculative suggestion, which calls for further investigation in the context of self-consistent formulations, where both the membrane and the genetic material are dynamically evolved.

It is clear that the work presented here can be extended in various ways. The nature of the lattice structure that is assumed can be generalized. For instance it is straightforward to include next-nearest neighbors, next-next nearest neighbors, and so on. The analytical treatment is analogous, and the results the same; only the form of the operator $\Delta_{\mathbf{k}}$ changes. Numerical simulations could also be performed in

higher dimensions. In particular, a toroidal (donutlike) cell embedded in a three-dimensional space can be straightforwardly simulated and analyzed. The inner volume of the cell is again partitioned into microcells, but now the constituents of all the microcells and not just those closest to the boundary, take part in the reactions. Distinct diffusion rates are assigned to the radial and longitudinal directions. Preliminary simulations indicate that collective modes can develop, giving rise to organized spatiotemporal dynamics [36] of a similar kind to those found in this paper. It would be interesting to extend this analysis to other geometries and make contact with work which assumes the oscillations to be present throughout the cell (see, for instance [37]).

APPENDIX A: THE VAN-KAMPEN EXPANSION

In this appendix we will give more details of the application of the van Kampen system-size expansion to the master Eq. (9). A general discussion of the method is given in van Kampen's book [24] and a description of the application to a simple model showing sustained and enhanced stochastic fluctuations is given in [25]. The calculations given below build upon those carried out for the nonspatial version of the model considered in this paper [23] and a spatial predator-prey model [28]. We will occasionally refer back to these two papers below.

The starting point for the expansion in powers of $N^{-1/2}$ is the ansatz [Eq. (14)]. From this the following two results can be derived [24]. First, the left-hand side of the master Eq. (9) is given by

$$\frac{dP(\mathbf{n},t)}{dt} = \frac{\partial\Pi(\xi_m^i,t)}{\partial t} - N^{1/2}\sum_{j=1}^{\Omega}\sum_{s=1}^{k}\frac{\partial\Pi(\xi_m^i,t)}{\partial\xi_s^j}\frac{d\phi_s^j}{dt}, \quad (A1)$$

where $\Pi(\xi_m^i,t) \equiv P(n_m^i,t)$. Second, the step operator $\mathcal{E}_{s,j}^{\pm 1}$ may be expanded:

$$\mathcal{E}_{s,j}^{\pm 1} = 1 \pm N^{-1/2}\frac{\partial}{\partial\xi_s^j} + (2N)^{-1}\frac{\partial^2}{\partial(\xi_s^j)^2} + \cdots$$

$$\equiv 1 \pm N^{-1/2}\partial_{\xi_s^j} + (2N)^{-1}\partial_{\xi_s^j}^2 + \cdots. \quad (A2)$$

The right-hand side of the master equation may be also expanded. We begin by defining new operators which are the coefficients of $N^{-1/2}$ and N^{-1} in the expansion of the particular combinations of the step operators which appear in the model. These are

$$(\mathcal{E}_{s,j}\mathcal{E}_{s+1,j}^{-1} - 1) \simeq N^{-1/2}(\partial_{\xi_s^j} - \partial_{\xi_{s+1}^j}) + \frac{1}{2}[N^{-1/2}(\partial_{\xi_s^j} - \partial_{\xi_{s+1}^j})]^2$$

$$\equiv N^{-1/2}\hat{L}_{1s} + \frac{1}{2}N^{-1}\hat{L}_{2s},$$

$$(\mathcal{E}_{s,j}\mathcal{E}_{s,j'}^{-1} - 1) \simeq N^{-1/2}(\partial_{\xi_s^j} - \partial_{\xi_s^{j'}}) + \frac{1}{2}[N^{-1/2}(\partial_{\xi_s^j} - \partial_{\xi_s^{j'}})]^2$$

$$\equiv N^{-1/2}\hat{L}_{1j} + \frac{1}{2}N^{-1}\hat{L}_{2j},$$

where the operators $\hat{L}_{1s}$ and $\hat{L}_{2s}$ read as

$$\hat{L}_{1s} = (\partial_{\xi_s^j} - \partial_{\xi_{s+1}^j}), \quad \hat{L}_{2s} = (\partial_{\xi_s^j} - \partial_{\xi_{s+1}^j})^2$$

and where $\hat{L}_{1j}$ and $\hat{L}_{2j}$ read as

$$\hat{L}_{1j} = (\partial_{\xi_s^j} - \partial_{\xi_s^{j'}}), \quad \hat{L}_{2j} = (\partial_{\xi_s^j} - \partial_{\xi_s^{j'}})^2.$$

In addition

$$(\mathcal{E}_{s,j}^{-1} - 1) \sim -N^{-1/2}\partial_{\xi_s^j} + \frac{1}{2}N^{-1}\partial_{\xi_s^j}^2,$$

$$(\mathcal{E}_{s,j} - 1) \sim N^{-1/2}\partial_{\xi_s^j} + \frac{1}{2}N^{-1}\partial_{\xi_s^j}^2.$$

For each of the three terms appearing in Eq. (9), namely, the local, migration, and environmental terms, we can now identify the various contributions in the van Kampen expansion: those of order $N^{-1/2}$, those of order N^{-1} involving a single derivative, and those of order N^{-1} but involving two derivatives. We will examine these in turn.

1. Right-hand side of the master equation: The $N^{-1/2}$ terms

The contribution from $\mathcal{T}_{\mathrm{loc}}^j$, defined by Eq. (11), is

$$\sum_s \frac{\eta_{s+1}}{\Omega}\hat{L}_{1s}(\phi_s^j\phi_{s+1}^j).$$

Using the definition of $\hat{L}_{1s}$, shifting the sum on s and remembering that quantities with subscripts $k+1$ are to be identified with those with subscripts 1, we obtain

$$\mathcal{T}_{\mathrm{loc}}^{j(1)} = \frac{1}{\Omega}\sum_s (\eta_{s+1}\phi_s^j\phi_{s+1}^j - \eta_s\phi_{s-1}^j\phi_s^j)\partial_{\xi_s^j}, \quad \text{(A3)}$$

where the superscript (1) indicates that this is only the contribution to $\mathcal{T}_{\mathrm{loc}}^j$ from terms of order $N^{-1/2}$. It should be noted that Eq. (A3) operates on $\Pi(\xi_m^i, t)$.

The contribution from $\mathcal{T}_{\mathrm{mig}}^{jj'}$, defined by Eq. (12) and using the definition of $\hat{L}_{1j}$, is

$$\frac{2}{z\Omega}\sum_s \alpha_s\partial_{\xi_s^j}\left[\phi_s^j\left(1 - \sum_m \phi_m^{j'}\right) - \phi_s^{j'}\left(1 - \sum_m \phi_m^j\right)\right].$$

To write this contribution in a way which naturally involves the Laplacian operator we add to this sum two terms which add to zero, namely,

$$0 = \phi_s^j\sum_m \phi_m^j - \phi_s^j\sum_m \phi_m^j.$$

Summing the contribution over $j' \in j$ and introducing the discrete Laplacian $\Delta f_s^j = (2/z)\sum_{j' \in j}(f_s^{j'} - f_s^j)$, we obtain

$$\sum_{j'} \mathcal{T}_{\mathrm{mig}}^{jj'(1)} = -\sum_s \frac{\alpha_s}{\Omega}\left[\Delta\phi_s^j\left(1 - \sum_m \phi_m^j\right) + \phi_s^j\sum_m \Delta\phi_m^j\right].$$

(A4)

The contribution from $\mathcal{T}_{\mathrm{env}}^j$, defined by Eq. (13), is immediately found to be

$$\mathcal{T}_{\mathrm{env}}^{j(1)} = \sum_s \left\{\frac{\partial}{\partial\xi_s^j}\left[\frac{\gamma_s}{\Omega}\phi_s^j - \frac{\beta_s}{\Omega}\left(1 - \sum_m \phi_m^j\right)\right]\right\}. \quad \text{(A5)}$$

Adding the three terms [Eq. (A3)–(A5)] together, and letting them act on $\Pi(\xi_m^i, t)$ and summing over j, we may equate the resulting expression to the order $N^{1/2}$ term in Eq. (A1), after the rescaling of time $\tau = t/(N\Omega)$. The resulting equation describes the deterministic time evolution of the species s in microcell j in the limit $N \to \infty$, and is given by Eq. (15) in the main text.

2. Right-hand side of the master equation: The N^{-1} terms with a single derivative

These contributions are expressed in terms of the operators $\hat{L}_{1s}$ and $\hat{L}_{1j}$ and so are a function of the first derivatives in the fluctuation variables. We proceed as we did for the terms of order $N^{-1/2}$.

The contribution from $\mathcal{T}_{\mathrm{loc}}^j$, defined by Eq. (11), is

$$\mathcal{T}_{\mathrm{loc}}^{j(2)} = \sum_{s=1}^k \frac{\eta_{s+1}}{\Omega}[\hat{L}_{1s}(\phi_s^j\xi_{s+1}^j + \phi_{s+1}^j\xi_s^j)]$$

$$= \frac{1}{\Omega}\sum_{s=1}^k \left\{\frac{\partial}{\partial\xi_s^j}[\phi_s^j(\eta_{s+1}\xi_{s+1}^j - \eta_s\xi_{s-1}^j)\right.$$

$$\left. + \xi_s^j(\eta_{s+1}\phi_{s+1}^j - \eta_s\phi_{s-1}^j)]\right\}, \quad \text{(A6)}$$

where once again use has been made of the definition $\hat{L}_{1s}$, the cyclic nature of the species, and the sum on s has been shifted. Here the superscript (2) indicates that this is only the contribution to $\mathcal{T}_{\mathrm{loc}}^j$ from terms of order N^{-1} with a single derivative.

The contribution from $\mathcal{T}_{\mathrm{mig}}^{jj'}$, defined by Eq. (12), is

$$\frac{2}{z\Omega}\sum_s \alpha_s\left\{\hat{L}_{1j}\left[\phi_s^j\left(-\sum_m \xi_m^{j'}\right) + \xi_s^j\left(1 - \sum_m \phi_m^{j'}\right)\right]\right\}.$$

Performing the same manipulations as before but also inserting the identities

$$0 = \xi_s^j\sum_m \phi_m^j - \xi_s^j\sum_m \phi_m^j, \quad 0 = \phi_s^j\sum_m \xi_m^j - \phi_s^j\sum_m \xi_m^j,$$

gives, after summing over $j' \in j$,

$$\sum_{j'} \mathcal{T}_{\mathrm{mig}}^{jj'(2)} = -\frac{1}{\Omega}\sum_s \alpha_s\left[\frac{\partial}{\partial\xi_s^j}\left(\Delta\xi_s^j + \xi_s^j\sum_m \Delta\phi_m^j - \Delta\phi_s^j\sum_m \xi_m^j\right.\right.$$

$$\left.\left. + \phi_s^j\sum_m \Delta\xi_m^j - \Delta\xi_s^j\sum_m \phi_m^j\right)\right]. \quad \text{(A7)}$$

Finally, the contribution from $\mathcal{T}_{\text{env}}^j$, defined by Eq. (13), is immediately found to be

$$\mathcal{T}_{\text{env}}^{j(2)} = \sum_s \left[\frac{\partial}{\partial \xi_s^j} \left(\frac{\gamma_s}{\Omega} \xi_s^j + \frac{\beta_s}{\Omega} \sum_m \xi_m^j \right) \right]. \quad \text{(A8)}$$

3. Right-hand side of the master equation: The N^{-1} terms with two derivatives

These terms are expressed in terms of the operator $\hat{L}_{2s}$ and $\hat{L}_{2j}$ and so are a function of the second-order derivatives in the fluctuation variables. We proceed as we did in the two previous cases.

The contribution from $\mathcal{T}_{\text{loc}}^j$ is

$$\mathcal{T}_{\text{loc}}^{j(3)} = \frac{1}{\Omega} \sum_s \eta_{s+1} \frac{1}{2} \hat{L}_{2s} (\phi_s^j \phi_{s+1}^j)$$

$$= \frac{1}{2\Omega} \sum_s \eta_{s+1} (\phi_s^j \phi_{s+1}^j) \left(\frac{\partial^2}{\partial (\xi_s^j)^2} + \frac{\partial^2}{\partial (\xi_{s+1}^j)^2} - 2 \frac{\partial^2}{\partial \xi_s^j \partial \xi_{s+1}^j} \right). \quad \text{(A9)}$$

The contribution from $\mathcal{T}_{\text{mig}}^{jj'}$ is

$$\mathcal{T}_{\text{mig}}^{jj'(3)} = \frac{1}{z\Omega} \sum_s \alpha_s \frac{1}{2} \left\{ \hat{L}_{2j} \left[\phi_s^j \left(1 - \sum_m \phi_m^{j'} \right) \right] \right\}$$

$$= \alpha_s \frac{1}{z\Omega} \sum_s \left[\phi_s^j \left(1 - \sum_m \phi_m^{j'} \right) \right] \left(\frac{\partial}{\partial \xi_s^j} - \frac{\partial}{\partial \xi_s^{j'}} \right)^2. \quad \text{(A10)}$$

Finally, the contribution from $\mathcal{T}_{\text{env}}^j$ is found to be

$$\mathcal{T}_{\text{env}}^{j(3)} = \frac{1}{2} \sum_s \left[\frac{\beta_s}{\Omega} \left(1 - \sum_m \phi_m^j \right) + \frac{\gamma_s}{\Omega} \phi_s^j \right] \frac{\partial^2}{\partial (\xi_s^j)^2}. \quad \text{(A11)}$$

Adding the six terms [Eqs. (A6)–(A11)] together and letting them act on $\Pi(\xi_m^i, t)$ and summing over j, we may equate the resulting expression to the order one term in Eq. (A1), after the rescaling of time $\tau = t/(N\Omega)$. The resulting equation gives the stochastic time evolution of the species s in microcell j. It takes the form of a Fokker-Planck equation which we now examine.

APPENDIX B: THE FORM OF THE MATRICES M AND $\mathcal{B}$

To write down the differential equation for $\Pi(\xi_s^j, \tau)$, it is convenient to combine the indices s and j, labeling the species and microcells, respectively, by a single index p. To do this we imagine the $k\Omega$-dimensional vector with components ξ_s^j as an ordered sequence of Ω vectors, each of k components. This can be achieved by defining $p = (j-1)k+s$ so that the component ξ_p represents the fluctuations associated with the sth species in the jth microcell.

Now the terms in Eqs. (A6)–(A8) take the form of a single derivative of ξ_p acting on a linear combination of ξ_l, $l = 1, \ldots, k\Omega$ and the terms in Eqs. (A9)–(A11) are a linear combination of second-order derivatives. Therefore

using this more compact notation the Fokker-Planck takes the form

$$\frac{\partial \Pi}{\partial \tau} = - \sum_p \frac{\partial}{\partial \xi_p} [\mathcal{A}_p(\boldsymbol{\xi}) \Pi] + \frac{1}{2} \sum_{l,p} \mathcal{B}_{lp} \frac{\partial^2 \Pi}{\partial \xi_l \partial \xi_p}, \quad \text{(B1)}$$

where the matrix $\mathcal{A}$ can be rewritten as

$$\mathcal{A}_p(\boldsymbol{\xi}) = \sum_l M_{pl} \xi_l. \quad \text{(B2)}$$

So to specify the Fokker-Planck equation we need to give the form of the two $(k\Omega) \times (k\Omega)$ matrices M and $\mathcal{B}$. We first note that although they do not depend on the fluctuations $\xi_p(\tau)$, they do depend on the solution of the deterministic differential Eq. (15), as well as on the reaction rates $\eta_s, \alpha_s, \beta_s$ and γ_s. However since we are only interested in the fluctuations about the stationary state ϕ^* given by Eq. (16) and since we obtained this solution under the assumption that η_s, β_s and γ_s were independent of s, we take the two matrices to only depend on $\phi^*, \eta, \beta, \gamma$ and α_s. An inspection of Eqs. (A6)–(A11) reveals that the only spatial dependence in M and $\mathcal{B}$ originates from the discrete Laplacian. This suggests that if we introduce spatial Fourier transforms, we should be able to diagonalize M and $\mathcal{B}$, and so be left with matrices only in the species space. This is most easily carried out by not continuing to work with the Fokker-Planck Eq. (B1) but instead with the equivalent Langevin equation [31,32];

$$\frac{d\xi_p}{d\tau} = \mathcal{A}_p(\boldsymbol{\xi}) + \lambda_p(\tau), \quad \text{(B3)}$$

where

$$\langle \lambda_p(\tau) \lambda_q(\tau') \rangle = \mathcal{B}_{pq} \delta(\tau - \tau') \quad \text{(B4)}$$

and where the noise term, $\lambda_p(\tau)$, in Eq. (B3) is Gaussian with zero mean. This is Eq. (17) in the main text, but using the single index notation.

We follow the conventions and methods of [28] for the spatial Fourier transforms. For simplicity, we shall assume that the lattice is a d-dimensional hypercubic lattice, with lattice spacing a. Then the Fourier transform, $f_s^{\mathbf{k}}$, of a function $f_s^{\mathbf{j}}$, is defined by

$$f_s^{\mathbf{k}} = a^d \sum_{\mathbf{j}} e^{-i\mathbf{k}.a\mathbf{j}} f_s^{\mathbf{j}}, \quad \text{(B5)}$$

where we have now written the lattice site label $\mathbf{j}$ as a vector to emphasize the d-dimensional nature of the transform. We may now take the spatial Fourier transform of the matrix M. Since the only spatial dependence is through the discrete Laplacian, we may decompose Eq. (B2) as follows:

$$A_s^{\mathbf{j}} = \sum_{\mathbf{j}'} \sum_r M_{sr}^{\mathbf{j}\mathbf{j}'} \xi_r^{\mathbf{j}'} = \sum_r [M_{sr}^{(NS)} \xi_r^{\mathbf{j}} + M_{sr}^{(SP)} \Delta \xi_r^{\mathbf{j}}], \quad \text{(B6)}$$

where the two $k \times k$ matrices $M^{(NS)}$ and $M^{(SP)}$ will be specified below. It is now straightforward to take the spatial Fourier transform of Eq. (B6) to obtain [28]

$$A_s^{\mathbf{k}} = \sum_r [M_{sr}^{(NS)} + M_{sr}^{(SP)} \Delta_{\mathbf{k}}] \xi_r^{\mathbf{k}}, \tag{B7}$$

where $\Delta_{\mathbf{k}}$ is the Fourier transform of the discrete Laplacian and is given by

$$\Delta_{\mathbf{k}} = \frac{2}{d} \sum_{\gamma=1}^{d} [\cos(k_\gamma a) - 1]. \tag{B8}$$

Care should be taken not to confuse the components of the wave vector $\mathbf{k}$ and k, the number of chemical species. We have denoted the γth component of the wave vector $\mathbf{k}$ by k_γ to help avoid this confusion.

The quantity within the square brackets in Eq. (B7) is the spatial Fourier transform of the matrix M. It is diagonal in $\mathbf{k}$ space and so depends on the single label $\mathbf{k}$. We may therefore write it as

$$M_{sr}^{\mathbf{k}} = M_{sr}^{(NS)} + M_{sr}^{(SP)} \Delta_{\mathbf{k}}, \tag{B9}$$

where the two matrices $M^{(NS)}$ and $M^{(SP)}$ may be read off from Eqs. (A6)–(A8) and are given by

$$M_{ss}^{(NS)} = -\beta - \gamma, \tag{B10}$$

$$M_{sr}^{(NS)} = \begin{cases} -\eta\phi^* - \beta, & \text{if } r = s+1 \\ \eta\phi^* - \beta, & \text{if } r = s-1 \\ -\beta, & \text{if } |s-r| > 1, \end{cases} \tag{B11}$$

and

$$M_{ss}^{(SP)} = \alpha_s[1 + (1-k)\phi^*], \tag{B12}$$

$$M_{sr}^{(SP)} = \alpha_s\phi^* \text{ if } s \neq r. \tag{B13}$$

The matrix $M^{(NP)}$ is exactly the one found in the nonspatial version of the model [23], which is why we have attached the label *NS* to it to signify the nonspatial contribution to M. The spatial or *SP* contribution is simply $M^{(SP)}\Delta_{\mathbf{k}}$.

To take the Fourier transform of the matrix $\mathcal{B}$, we note that out of the three terms—given by Eqs. (A9)–(A11)—from which this matrix is constructed, the only nontrivial

spatial dependence comes from Eq. (A10). We display the contribution containing this dependence by noting the following relation:

$$\sum_{\mathbf{j}} \sum_{\mathbf{j}' \in \mathbf{j}} \left[\frac{\partial}{\partial \xi_s^{\mathbf{j}}} - \frac{\partial}{\partial \xi_s^{\mathbf{j}'}} \right]^2$$
$$= 2\sum_{\mathbf{j}} \sum_{\mathbf{j}'} \left[z\frac{\partial^2}{\partial(\xi_s^{\mathbf{j}})^2}\delta_{\mathbf{jj}'} - \frac{\partial^2}{\partial\xi_s^{\mathbf{j}}\partial\xi_s^{\mathbf{j}'}}J_{\langle\mathbf{jj}'\rangle} \right], \quad \text{(B14)}$$

where $J_{\langle\mathbf{jj}'\rangle}$ is equal to 1 if $\mathbf{j}'$ and $\mathbf{j}$ are nearest neighbors and zero otherwise. The part of the $\mathcal{B}$ matrix corresponding to expression (B14) is $(2z\delta_{\mathbf{jj}'} - 2J_{\langle\mathbf{jj}'\rangle})$ which has Fourier transform

$$a^d\left[2z - 4\sum_{\gamma=1}^{d}\cos(k_\gamma a) \right] = -za^d\Delta_{\mathbf{k}},$$

using Eq. (B8) and $z=2d$. Therefore we may express the matrix $\mathcal{B}$ in Fourier space in a similar way to Eq. (B9):

$$\mathcal{B}_{sr}^{\mathbf{k}} = \mathcal{B}_{sr}^{(NS)} + \mathcal{B}_{sr}^{(SP)}\Delta_{\mathbf{k}}, \tag{B15}$$

where the two $k \times k$ matrices $\mathcal{B}^{(NS)}$ and $\mathcal{B}^{(SP)}$ may be read off from Eqs. (A9)–(A11) and are given by

$$\mathcal{B}_{ss}^{(NS)} = a^d[\beta(1-k\phi^*) + \gamma\phi^* + 2\eta(\phi^*)^2], \tag{B16}$$

$$\mathcal{B}_{sr}^{(NS)} = \begin{cases} -a^d\eta(\phi^*)^2, & \text{if } r = s+1 \\ -a^d\eta(\phi^*)^2, & \text{if } r = s-1 \\ 0 & \text{if } |s-r| > 1, \end{cases} \tag{B17}$$

and

$$\mathcal{B}_{ss}^{(SP)} = -2a^d\alpha_s\phi^*(1-k\phi^*), \tag{B18}$$

$$\mathcal{B}_{sr}^{(SP)} = 0 \text{ if } s \neq r. \tag{B19}$$

Once again, the matrix $\mathcal{B}^{(NS)}$ is exactly the one found in the nonspatial version of the model [23], up to a factor of a^d, which is why we have attached the label *NS* to it. The spatial contribution is $\mathcal{B}^{(SP)}\Delta_{\mathbf{k}}$.

---

[1] B. Alberts *et al.*, *Molecular Biology of the Cell*, 5th ed. (Garland Science, New York, 2007).

[2] D. W. Deamer, Origins Life Evol. Biosphere **17**, 3 (1986).

[3] H. J. Morowitz, B. Heinz, and D. W. Deamer, Origins Life Evol. Biosphere **18**, 281 (1988).

[4] G. Ourisson and Y. Nakatani, Tetrahedron **55**, 3183 (1999).

[5] J. W. Szostak, D. P. Bartel, and P. L. Luisi, Nature (London) **409**, 387 (2001).

[6] S. Rasmussen *et al.*, Science **303**, 963 (2004).

[7] I. A. Chen, R. W. Roberts, and J. W. Szostak, Science **305**, 1474 (2004).

[8] P. Stano and P. L. Luisi, Origins Life Evol. Biosphere **37**, 303 (2007).

[9] D. Deamer, Prog. Theor. Phys. Suppl. **173**, 11 (2008).

[10] S. Rasmussen *et al.*, *Protocells: Bridging Nonliving and Living*

Matter (MIT Press, Cambridge, MA, 2008).

[11] P. L. Luisi, *The Emergence of Life* (Cambridge University Press, Cambridge, 2006).

[12] U. Seifert, Adv. Phys. **46**, 13 (1997).

[13] P. Gray and S. K. Scott, J. Phys. Chem. **89**, 22 (1985).

[14] F. Dyson, *Origins of Life* (Cambridge University Press, Cambridge, England, 1985).

[15] S. A. Kauffman, J. Theor. Biol. **119**, 1 (1986); *The Origins of Order* (Oxford University Press, Oxford, 1993).

[16] P. F. Stadler and P. Schuster, Bull. Math. Biol. **52**, 485 (1990).

[17] G. Wächtershäuser, Proc. Natl. Acad. Sci. U.S.A. **87**, 200 (1990).

[18] S. Jain and S. Krishna, Phys. Rev. Lett. **81**, 5684 (1998).

[19] M. Eigen, Naturwiss. **58**, 465 (1971).

[20] H. Lodish *et al.*, *Molecular Cell Biology*, 6th ed. (W. H.

Freeman and Co., New York, 2008).

[21] Y. Togashi and K. Kaneko, Phys. Rev. Lett. **86**, 2459 (2001).

[22] Y. Togashi and K. Kaneko, J. Phys. Soc. Jpn. **72**, 62 (2003).

[23] T. Dauxois, F. Di Patti, D. Fanelli, and A. J. McKane, Phys. Rev. E **79**, 036112 (2009).

[24] N. G. van Kampen, *Stochastic Processes in Physics and Chemistry*, 3rd ed. (Elsevier, Amsterdam, 2007).

[25] A. J. McKane and T. J. Newman, Phys. Rev. Lett. **94**, 218102 (2005).

[26] A. J. McKane, J. D. Nagy, T. J. Newman, and M. O. Stefanini, J. Stat. Phys. **128**, 165 (2007).

[27] D. Alonso, A. J. McKane, and M. Pascual, J. R. Soc., Interface **4**, 575 (2007).

[28] C. A. Lugo and A. J. McKane, Phys. Rev. E **78**, 051911 (2008).

[29] D. T. Gillespie, J. Comput. Phys. **22**, 403 (1976).

[30] D. T. Gillespie, J. Phys. Chem. **81**, 2340 (1977).

[31] C. W. Gardiner, *Handbook of Stochastic Methods*, 3rd ed. (Springer-Verlag, Berlin, 2004).

[32] H. Risken, *The Fokker-Planck Equation*, 2nd ed. (Springer-Verlag, Berlin, 1989).

[33] D. Fanelli and A. J. McKane, Phys. Rev. E **78**, 051406 (2008).

[34] J. Macía and R. V. Solé, J. Theor. Biol. **245**, 400 (2007).

[35] J. Macía and R. V. Solé, Philos. Trans. R. Soc. London, Ser. B **362**, 1821 (2007).

[36] F. Di Patti, T. Dauxois, P. de Anna, D. Fanelli, and A. J. McKane. HCP-Europa 2, Final Report (2010).

[37] V. P. Zhdanov, Phys. Chem. Chem. Phys. **2**, 5268 (2000).